Opposing reactions in coenzyme A metabolism sensitize *Mycobacterium tuberculosis* to enzyme inhibition

Elaine Ballinger*, John Mosior*, Travis Hartman, Kristin Burns-Huang, Ben Gold, Roxanne Morris, Laurent Goullieux, Isabelle Blanc, Julien Vaubourgeix, Sophie Lagrange, Laurent Fraisse, Stéphanie Sans, Cedric Couturier, Eric Bacqué, Kyu Rhee, Sarah M. Scarry, Jeffrey Aubé, Guangbin Yang, Ouathek Ouerfelli, Dirk Schnappinger, Thomas R. Ioerger, Curtis A. Engelhart, Jennifer A. McConnell, Kathrine McAulay, Allison Fay, Christine Roubert, James Sacchettini†‡, Carl Nathan†‡

INTRODUCTION: *Mycobacterium tuberculosis* (Mtb) is the leading global cause of lethal infection in humans and accounts for the largest number of drug-resistant infections by a single bacterial pathogen. Resistance is particularly high against the most widely prescribed tuberculosis (TB) drug, isoniazid. Isoniazid blocks synthesis of mycolates, ultralong-chain fatty acids that provide structure to the waxy coat that surrounds Mtb cells and are incorporated into some of its virulence lipids. There is currently no known method to block the synthesis of both mycolates and nonmycolate-containing virulence lipids of Mtb at a single point of control. One such control point is phosphopantetheinyl transferase (PptT). PptT transfers 4′-phosphopantetheine (Ppt) from coenzyme A (CoA) to acyl carrier proteins (ACPs) that synthesize the lipids critical to Mtb structural integrity and virulence.

RATIONALE: TB drug discovery often begins with whole-cell, high-throughput screens that yield compounds that kill Mtb by unknown means. Selection of Mtb mutants resistant to these compounds can indicate candidate targets of the active compound, but experimental validation is required to confirm the functionally relevant target, which is often an enzyme. A suitable target must be essential in vivo, such that its inhibition precludes development of TB in animal models, but also "vulnerable," meaning that a pharmacologically attainable level of inhibition should be lethal to Mtb within a patient. The inhibitor should act only on Mtb, and resistance should be rare.

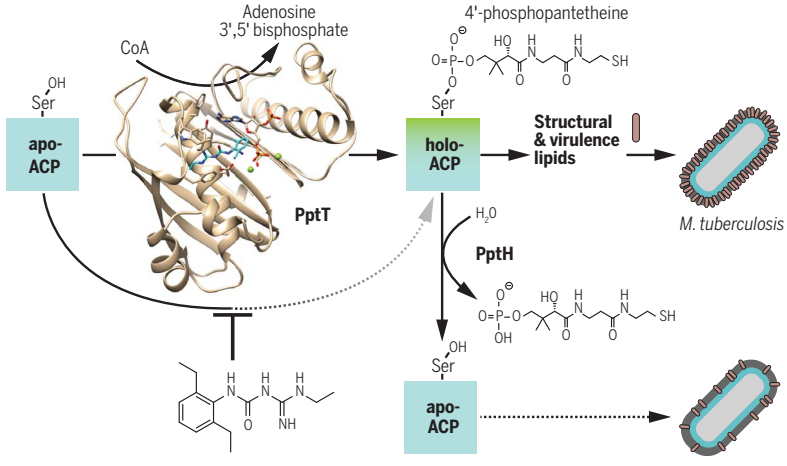

The enzymes PptT and PptH have been found to perform opposing reactions in Mtb lipid metabolism, an essential process demonstrated to be a target for drug development. PptT transfers 4′-phosphopantetheine (Ppt) from CoA to apo-acyl carrier proteins (Apo-ACP) in Mtb, generating holo-ACPs that help synthesize structural and virulence lipids. Compound 8918 binds to the Ppt binding pocket of PptT, displacing the Ppt arm of CoA and partially inhibiting this enzyme. The Ppt hydrolase PptH can release Ppt, regenerating apo-ACP and thus sensitizing Mtb cells to inhibition of PptT.

RESULTS: Screening a chemical library revealed an amidino-urea compound called "8918" that kills Mtb, including drug-resistant clinical isolates. 8918 inhibits Mtb in mice and spares other bacteria, yeast, and mammalian cells.

Rare Mtb mutants resistant to 8918 bore a point mutation in the PptT gene *rv2794c*, altering an amino acid residue overlying the Ppt-binding pocket of PptT. When Mtb carried the mutant allele as an extra copy of *rv2794c*, the Mtb was protected from 8918. 8918 inhibited recombinant PptT, albeit noncompetitively and incompletely. The impact of 8918 on the Mtb metabolome and lipids was consistent with inhibition of PptT in the intact cell. A crystal structure of the PptT-8918 complex at 1.8-Å resolution confirmed that 8918 binds within the Ppt binding pocket, adjacent to the phosphoadenosine phosphate portion of CoA. Intact CoA remained in the PptT-8918 complex, but the Ppt arm was displaced, decreasing but not abolishing PptT's catalytic activity. Strains of Mtb producing reduced amounts of PptT became hypersensitive to 8918.

ON OUR WEBSITE

Read the full article at http://dx.doi.org/10.1126/science.aau8959

It was puzzling that even partial inhibition of PptT killed Mtb. We observed that mutants with disruption of *rv2795c*, a gene encoding a hypothetical protein, were also highly resistant to 8918. Recombinant Rv2795c protein hydrolyzed Ppt from a mycolate-building holo-ACP that is a substrate for PptT. The action of this Ppt hydrolase (PptH) resembled that of nonhomologous enzymes called ACP hydrolases that remove Ppt from ACPs in vitro but whose physiological function is unknown.

CONCLUSION: We identified a small molecule that kills Mtb by inhibiting PptT, demonstrating that a key enzyme in CoA metabolism is a viable target for TB drug development. Even partial inhibition of PptT is toxic to Mtb, likely because PptH synergizes with the inhibitor by undoing the PptT reaction. PptT and PptH are co-regulated by translation from the same operon, and thus Mtb cannot respond to inhibition of PptT by making more PptT without also generating more PptH. The joint functioning of PptT and PptH suggests that Mtb closely regulates the activation of ACPs. The transcriptional co-regulation and constitutive function of both members of the PptT-PptH couple suggests that a posttranslational signal that impairs PptT more than PptH could allow Mtb to rapidly reverse a prior commitment to synthesis of its metabolically most costly lipids.

The list of author affiliations is available in the full article online.
*These authors contributed equally to this work.
†These authors contributed equally to this work.
‡Corresponding author. Email: cnathan@med.cornell.edu (C.N.); sacchett@tamu.edu (J.S.)
Cite this article as E. Ballinger *et al.*, *Science* **363**, eaau8959 (2019). DOI: 10.1126/science.aau8959

Opposing reactions in coenzyme A metabolism sensitize *Mycobacterium tuberculosis* to enzyme inhibition

Elaine Ballinger[1]*, John Mosior[2]*, Travis Hartman[3], Kristin Burns-Huang[1], Ben Gold[1], Roxanne Morris[3], Laurent Goullieux[4]†, Isabelle Blanc[4]†, Julien Vaubourgeix[1], Sophie Lagrange[4]†, Laurent Fraisse[4]†, Stéphanie Sans[4]†, Cedric Couturier[4]†, Eric Bacqué[4]†, Kyu Rhee[3], Sarah M. Scarry[5], Jeffrey Aubé[5], Guangbin Yang[6], Ouathek Ouerfelli[6], Dirk Schnappinger[1], Thomas R. Ioerger[1], Curtis A. Engelhart[1], Jennifer A. McConnell[1], Kathrine McAulay[1], Allison Fay[8], Christine Roubert[4]†, James Sacchettini[2]‡§, Carl Nathan[1]‡§

Mycobacterium tuberculosis (Mtb) is the leading infectious cause of death in humans. Synthesis of lipids critical for Mtb's cell wall and virulence depends on phosphopantetheinyl transferase (PptT), an enzyme that transfers 4′-phosphopantetheine (Ppt) from coenzyme A (CoA) to diverse acyl carrier proteins. We identified a compound that kills Mtb by binding and partially inhibiting PptT. Killing of Mtb by the compound is potentiated by another enzyme encoded in the same operon, Ppt hydrolase (PptH), that undoes the PptT reaction. Thus, loss-of-function mutants of PptH displayed antimicrobial resistance. Our PptT-inhibitor cocrystal structure may aid further development of antimycobacterial agents against this long-sought target. The opposing reactions of PptT and PptH uncover a regulatory pathway in CoA physiology.

Beginning ~80 years ago, the "golden age" of antibiotic development led to a plethora of drugs that inhibited four classes of targets: enzymes involved in the synthesis of nucleic acids, proteins, cell walls, or folate (*1*). With antimicrobial resistance rising to the level of a global health emergency (*2*, *3*) and with tuberculosis (TB) being the leading cause of death from infectious disease (*3*), investigators have sought to develop whole-cell–active inhibitors of a wider range of mycobacterial targets, including enzymes involved in the synthesis of cofactors such as coenzyme A (CoA) (*4*–*7*).

An estimated 9% of 3500 known enzyme reactions depend on CoA (*7*), an evolutionarily conserved cofactor formed from the phosphoadenylation of 4′-phosphopantetheine (Ppt). Ppt's sulfhydryl group forms thioester bonds upon acylation, enabling the synthesis of complex lipids when Ppt is enzymatically transferred from CoA to apo-acyl carrier proteins (ACPs). *Mycobacterium tuberculosis* (Mtb) encodes two enzymes that catalyze the conversion of apo- to holo-ACPs via transfer of Ppt from CoA onto the carrier protein: Ppt transferase (PptT) and ACP synthase (AcpS). PptT and AcpS do not share substantial similarity at sequence or structural levels (*8*–*10*), and they activate different sets of ACPs. PptT, encoded by *rv2794c*, charges ACPs for the synthesis of structural lipids—mycolic acids of the cell wall—and virulence lipids, such as phthiocerol dimycoserosates (PDIMs) that suppress host immune reactions (*10*–*12*). PptT is essential to Mtb both in vitro and during infection in mice (*13*).

Both the synthesis of CoA and the transfer of Ppt have been targets of extensive drug development efforts (*4*, *14*, *15*), but no compounds have been reported that are bactericidal to wild-type (WT) Mtb through inhibition of these pathways. Here we report the discovery of a druglike amidinourea compound that kills Mtb by binding PptT, spares other bacteria and mammalian cells, and blocks growth of Mtb in the mouse. Analysis of resistant mutants led to the discovery of an enzyme, a Ppt hydrolase (PptH), whose loss of function (LOF) represents a new mechanism of antimicrobial resistance.

Identification of a mycobactericidal amidino-urea compound

A screen of more than 90,000 compounds representative of the Sanofi collection of small molecules identified the amidino-urea 1-[(2,6-diethylphenyl)-3-*N*-ethylcarbamimodoyl]urea, hereafter called "8918" (Fig. 1A). 8918 had an MIC_{90} (the minimum concentration tested that inhibited growth by ≥90%) of 3.1 μM against a lab strain of Mtb that is virulent in mice (H37Rv) (Table 1). MIC_{90}s varied no more than twofold when the carbon source was changed from the standard combination of glucose plus glycerol to glucose, glycerol, acetate, or cholesterol. The MIC_{90}s ranged from 0.56 to 3.0 μM (median, 1.5 μM) against 29 clinical isolates of Mtb, 14 of which were resistant to one or more of nine TB drugs and three of which were individually resistant to three, four, or six drugs, respectively (table S1), suggesting that 8918 was inhibiting a distinct target. 8918 reduced the colony-forming units (CFU) of Mtb H37Rv from

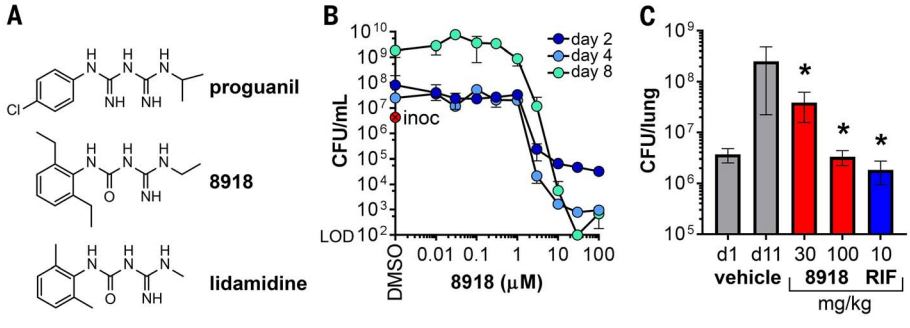

Fig. 1. Antimycobacterial activity of 8918 in vitro and in mice. (**A**) Structures of proguanil, 8918, and lidamidine. (**B**) In vitro activity against Mtb H37Rv. The plot shows colony-forming units (CFU) remaining after treatment with 8918. Inoc, inoculum at day 0. Results are means ± SD of triplicates in one experiment representative of three. DMSO, dimethyl sulfoxide. (**C**) In vivo activity against Mtb H37Rv. The histogram represents $\log_{10}$ CFU from the lungs of BALB/c mice. One day after intranasal inoculation of 10^6 Mtb H37Rv Mtb, mice were treated via oral gavage, 4 days per week for 2 weeks and then euthanized. Results are means ± SD for five mice per group in one experiment representative of two. Results for the 8918-treated groups were statistically significantly different than for the vehicle-treated group (*$P < 0.001$; one-way ANOVA).

[1]Department of Microbiology and Immunology, Weill Cornell Medicine, New York, NY, USA. [2]Departments of Biochemistry and Biophysics, Texas Agricultural and Mechanical University, College Station, TX, USA. [3]Department of Medicine, Weill Cornell Medicine, New York, NY, USA. [4]Infectious Diseases Therapeutic Area, Sanofi, Marcy-l'Étoile, France. [5]Division of Chemical Biology and Medicinal Chemistry, UNC Eshelman School of Pharmacy, University of North Carolina, Chapel Hill, NC, USA. [6]Organic Synthesis Core, Memorial Sloan Kettering Cancer Center, New York, NY, USA. [7]Department of Computer Science and Engineering, Texas Agricultural and Mechanical University, College Station, TX, USA. [8]Immunology Program, Sloan Kettering Institute, Memorial Sloan Kettering Cancer Center, New York, NY, USA.
*These authors contributed equally to this work.
†Present address: Evotec ID (Lyon) SAS, Marcy-l'Étoile, France.
‡These authors contributed equally to this work.
§Corresponding author. Email: cnathan@med.cornell.edu (C.N.); sacchett@tamu.edu (J.S.)

Table 1. 8918-resistant mutants of Mtb. MIC_{90} (micromolar units) of 8918, proguanil, lidamidine, isoniazid (INH), para-aminosalicyclic acid (PAS), rifampicin (RIF), ethambutol (EMB), and moxifloxacin (MOXI). Strains in bold were used in subsequent studies as representative strains for their respective mutations. Mutations in strains A1, A4, A6, B1, B2, B3, B4, and B5 were detected by whole-genome resequencing. The other mutations were found by Macrogen sequencing of the polymerase chain reaction–amplified gene. NT, not tested. Single-letter abbreviations for amino acid residues: A, Ala; D, Asp; E, Glu; F, Phe; G, Gly; H, His; L, Leu; N, Asn; R, Arg; S, Ser; V, Val; and W, Trp.

Strain	8918	Proguanil	Lidamidine	INH	PAS	RIF	EMB	MOXI	Mutation
WT	3.13	>100	>100	0.39	<0.05	0.1	6.25	<0.02	none
A1	**>100**	**>100**	**>100**	**0.39**	**<0.05**	**0.2**	**3.13**	**<0.02**	***rv2795c* H246N**
A2	>100	NT	NT	0.39	<0.05	0.1	3.13	<0.02	*rv2795c* H246N
A3	>100	NT	NT	0.39	<0.05	0.1	6.25	<0.02	*rv2795c* H246N
A4	**>100**	**>100**	**>100**	**0.39**	**<0.05**	**0.1**	**6.25**	**<0.02**	***pptT* W170S**
A5	>100	NT	NT	0.39	<0.05	0.2	6.25	<0.02	*rv2795c* V203F
A6	>100	NT	NT	0.39	0.1	0.2	6.25	<0.02	*rv2795c* V203F
B1	100	NT	NT	0.39	0.1	0.2	6.25	<0.02	*pptT* W170L
B2	>100	NT	NT	1.56	0.20	0.2	6.25	<0.02	*rv2795c* G266V
B3	>100	NT	NT	0.39	0.1	0.1	6.25	<0.02	*rv2795c* R321R, H246N
B4	>100	NT	NT	0.39	0.20	0.2	6.25	0.04	*rv2795c* D51E
B5	>100	NT	NT	0.39	0.1	0.1	6.25	<0.02	*rv2795c* H24N
B6	>100	NT	NT	0.39	<0.05	0.1	6.25	<0.02	*rv2795c* D137G

10^6 per ml to less than the limit of detection within 8 days (Fig. 1B). The compound closely resembles proguanil, a U.S. Food and Drug Administration–approved drug that inhibits the folate pathway in malaria parasites (Fig. 1A). Proguanil and its active form, cycloguanil (fig. S1), were inactive on Mtb, and 8918 did not appear to act by impairing Mtb's folate synthesis (fig. S2). Lidamidine, an antidiarrheal drug, also resembles 8918 (Fig. 1A) but was poorly active on Mtb (MIC_{90} >100 μM; MIC_{50} = 125 μM). The MBC_{99} of 8918 (the minimum concentration tested that was bactericidal for ≥99% of the bacteria) was 6.25 μM against Mtb and 3.13 μM against *Mycobacterium smegmatis*. In contrast, 8918 was inactive against *Staphylococcus aureus*, *Escherichia coli*, *Pseudomonas aeruginosa*, four species of *Streptomyces*, and *Candida albicans* and was noncytotoxic to human hepatoma cells (table S2).

After oral administration to mice of 100 mg/kg 8918 (i.e., 100 mg of 8918 per kilogram of body weight) in 0.6% methylcellulose/Tween 80 (99.5/0.5, vol/vol), the compound was bioavailable with a peak blood level of 2230 ng/ml at 0.25 hours, but the half-life was brief (6.7 hours) in association with rapid microsomal metabolism, a liability being addressed in ongoing studies. Nonetheless, accumulation in lung was 42 times that in plasma (9200 ng·hour/ml), encouraging us to test in vivo efficacy. In BALB/c mice infected intranasally with 10^6 Mtb H37Rv, oral administration of 8918 at 100 mg/kg per day and 4 days per week for eight doses prevented the replication of Mtb in the lungs as effectively as rifampin (10 mg/kg) dosed on the same schedule (Fig. 1C).

To further explore 8918's mode of action, we compared its impact on the Mtb metabolome with that of proguanil and four TB drugs with known targets: isoniazid, an inhibitor of a 2-trans-enoyl-ACP reductase in mycolic acid synthesis; streptomycin, an inhibitor of the ribosome; rifampin, an inhibitor of RNA polymerase; and para-aminosalicylic acid, an inhibitor of folate synthesis. We exposed a mat of Mtb on a filter to 20 μM 8918 in the underlying agar. Under these conditions, this concentration of 8918 does not halt growth of the bacterial population, which is at a cell density >10^3 higher than the standard conditions for MIC determination and which grew further over a week before addition of 8918 (fig. S3). We assayed the cells after a 24-hour exposure to 8918 to focus on primary rather than secondary effects, and we observed marked changes in abundance of CoA and precursors 4′-phosphopantothenate, pantetheine, 4′-phosphopantothenoylcysteine, and 4′-phosphopantetheine (Fig. 2A). At 48 hours, we also tested the impact of lidamidine and proguanil, which accumulated in Mtb to levels 9 and 10 times that of 8918, respectively (fig. S4). Of 37 metabolites in a discriminatory panel, concentration-responsive changes specific to 8918 and not proguanil were seen in three metabolites in the CoA path (propionyl/propanoyl CoA, 2-dehydropantolactone, and 3-hydroxypropionyl-CoA) and two metabolites whose production involves CoA (methyl citrate and malate), whereas (*R*)-pantoate levels declined and CoA was no longer depleted (fig. S5, A to F). Even though the importance of increases or decreases in specific pool sizes cannot be interpreted without flux analyses, the observed changes serve as a qualitative flag for affected pathways and bore little resemblance to the metabolomic effect of the four clinically used TB drugs (*16*) (fig. S6).

To summarize, 8918 is a druglike, noncytotoxic, narrow-spectrum mycobactericidal compound with whole-cell activity in axenic culture and efficacy in mice, whose target(s) seemed likely to be distinct from the targets of many TB drugs and to be related to the formation or use of CoA. These findings encouraged us to isolate spontaneous resistant mutants for target identification.

Two classes of mutants resistant to 8918

The frequency of resistance of Mtb H37Rv to 8918 at four times the MIC_{90} was 3×10^{-7}, comparable to the values for clinically used TB drugs; no mutants could be isolated at eight times the MIC_{90}. We isolated 12 resistant clones. All had MIC_{90}s > 100 μM in response to 8918 but were as sensitive as WT Mtb to rifampin, isoniazid, and ethambutol (Table 1).

Whole-genome resequencing identified two genes whose single-nucleotide polymorphisms were candidates for mediating resistance. The less frequently mutated gene (2 of 12 clones) was *rv2794c*, encoding PptT. Most of the resistant clones (10 of 12 with seven distinct mutations) were mutated in *rv2795c*, a gene adjacent to *pptT* in the same operon. Moreover, we isolated 12 8918-resistant clones of *M. smegmatis*, and all were point mutants or deletion mutants in the homolog of *rv2795c*. *rv2795c* encodes a protein of unknown function that is conserved among mycobacterial species. Because *rv2795c* has been characterized as nonessential (*17*), it was unlikely to encode the target. In contrast, because PptT is essential in Mtb (*13*), it was a candidate for being the target. Thus, our next step was to confirm whether PptT was indeed the target of 8918.

Effect of 8918 on Mtb lipids

An inhibitor of PptT would impair the conversion of apo-ACPs to holo-ACPs for the synthesis of mycolates and PDIMs, among other lipids (*13*). Consistent with this finding, thin-layer chromatography (TLC) analysis of mycobacteria labeled with ^{14}C-acetate or ^{14}C-propionate demonstrated marked 8918-mediated impairment of the synthesis of trehalose dimycolates (TDMs), trehalose monomycolates (TMMs), and PDIMs. Isoniazid, as expected, inhibited synthesis of TDMs and TMMs but not PDIMs. Proguanil had no observable effect on the mycolates or PDIMs (Fig. 2, B to D).

For a wider survey, we undertook a lipidomic analysis of 8918's effect on intact Mtb, again by using a 24-hour exposure at a concentration (20 μM) that, as noted, was sublethal for a dense mycobacterial mat on a filter, as reflected by the cells' continued growth. In the absence of new synthesis, replication could favor the loss of slow-turnover lipids by dilution. In contrast to the effect of 8918 on the de novo synthesis of certain lipids, the impact of a brief, sublethal exposure to 8918 on the abundance of lipid species was complex and variable across experiments, overlapping in part with the response to isoniazid, which was consistently observed (fig. S7 and table S3). In any one experiment, exposure to 8918 appeared to affect fewer than 5% of the 8954 features [discrete ion count peaks with a distinctive retention time and mass/charge (*m/z*) ratio] revealed by mass spectrometry (MS) of Mtb lipid extracts (fig. S8). Some of these changes may have reflected regulatory responses to 8918's depletion of CoA, as well as turnover of compound lipids,

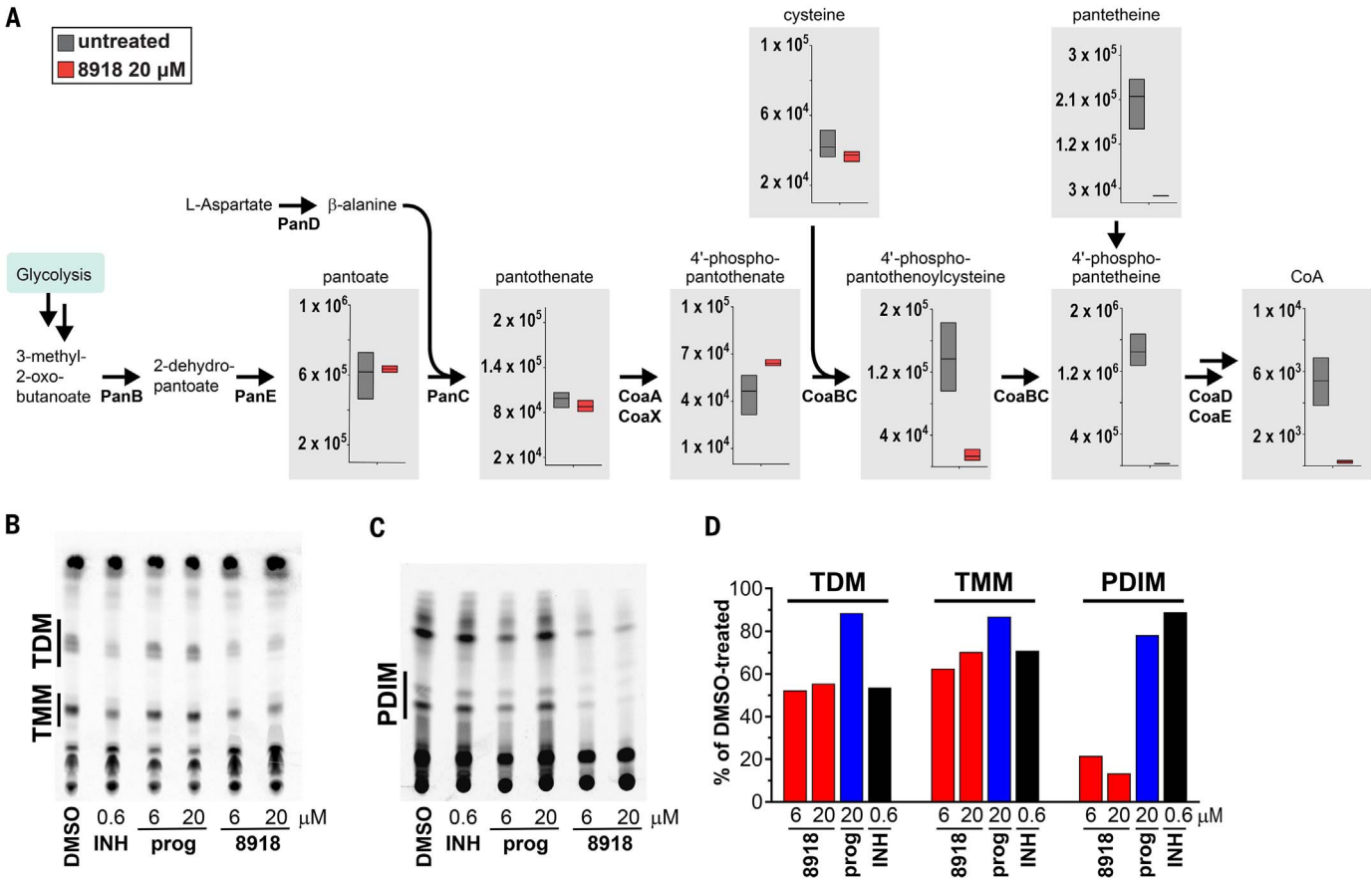

Fig. 2. Effect of 8918 on Mtb metabolites and lipids. (**A**) Impact on metabolites. Filter-grown Mtb was transferred to plates containing 7H9 medium with or without 8918 and lysates collected 24 hours later for LC-MS. The *y* axis indicates raw intensity values for the area under the curve for each metabolite peak. Boxes represent the range of peak areas of triplicate samples, and the center bar represents the median raw intensity value for each metabolite peak. (**B**) Impact on synthesis of TDMs and TMMs. *M. bovis* var. BCG was incubated with DMSO vehicle alone, isoniazid (INH, 0.6 μM), proguanil (prog, 6.25 or 20 μM), or 8918 (6.25 or 20 μM) for 12 hours, then exposed to ^{14}C acetate for 24 hours. Extracted lipids were subjected to TLC as described (*30*) (24-hour Phosphorimager exposure). (**C**) Impact on synthesis of PDIMs. The experiments were performed as described in (B) but using ^{14}C propionate (5-day Phosphorimager exposure). (**D**) Quantitation of results from (B) and (C) (24-hour exposures for both). Results for (A) to (D) are each from one experiment representative of two independent experiments.

resulting in an apparent increase in the levels of some of their preformed components.

In all, the effect of 8918 on synthesis of TDMs, TMMs, and PDIMs was consistent with inhibition of PptT in the intact cell. However, neither the metabolomic nor the lipid synthesis studies excluded the possibility that there might be other targets of 8918, nor did these analyses establish whether PptT was the functionally relevant target for 8918's ability to kill Mtb.

Confirmation that PptT is the functionally relevant target of 8918

Two independent point mutants in PptT conferred high-level resistance to 8918 (Table 1), and introduction of the resistance-associated allele $pptT_{W170S}$ (W170S, Trp^{170}→Ser) into WT Mtb conferred high-level resistance on the WT strain (Fig. 3A). These results established the functional relevance of PptT as a target of 8918 and showed that the resistance allele is dominant. Moreover, we confirmed that four Mtb strains made selectively hypomorphic for PptT to different degrees (*18*–*20*) were more susceptible to 8918 in proportion to the strength of suppression of PptT expression than the same strains expressing WT levels of PptT (Fig. 3, B and C). A similarly heightened susceptibility upon suppression of PptT was not seen with 19 other anti-infective agents (Fig. 3D and fig. S9).

8918 inhibits purified PptT and binds the Ppt pocket in the active site

To learn whether 8918 can inhibit PptT and if so by what mechanism, we purified recombinant Mtb PptT and gauged its activity by its ability to transfer 4′-phosphopantetheine and thereby activate a nonribosomal peptide synthetase that generates a colored product in the presence of adenosine triphosphate (ATP) and L-glutamine (*21*, *22*). Kinetic analysis of purified PptT showed an apparent Michaelis constant (K_m) for CoA that rose only slightly with increasing concentrations of 8918, whereas the apparent maximum rate of reaction (V_{max}) declined (Fig. 4A). Although 8918 inhibited PptT with an IC_{50} (median inhibitory concentration) of 2.5 μM (Fig. 4B), inhibition plateaued below 90% (Fig. 4, A and B). Thus, inhibition of PptT by 8918 was noncompetitive and partial (fig. S10A). The kinetics was unaffected by preincubating PptT with 8918 (fig. S10B). The K_m (with respect to CoA) of the resistant mutant PptT (W170S) was similar to that of the WT, although the catalytic rate (K_{cat}) and K_{cat}/K_m were reduced compared with those of the WT enzyme (K_{cat} of 30 versus 119 hour^{-1}; K_{cat}/K_m of 53 versus 198 μM^{-1} hour^{-1}) (fig. S10, C and D). Compound 8918 had no effect on the enzyme used in the second stage of the PptT assay (fig. S10E).

To understand inhibition of PptT by 8918 at the atomic level, we crystallized Mtb PptT in the presence of 8918 and refined the structure to 1.76-Å resolution (table S4) (PDB 6CT5). There were two copies of the enzyme in the crystal's asymmetric unit (fig. S11), each monomer of

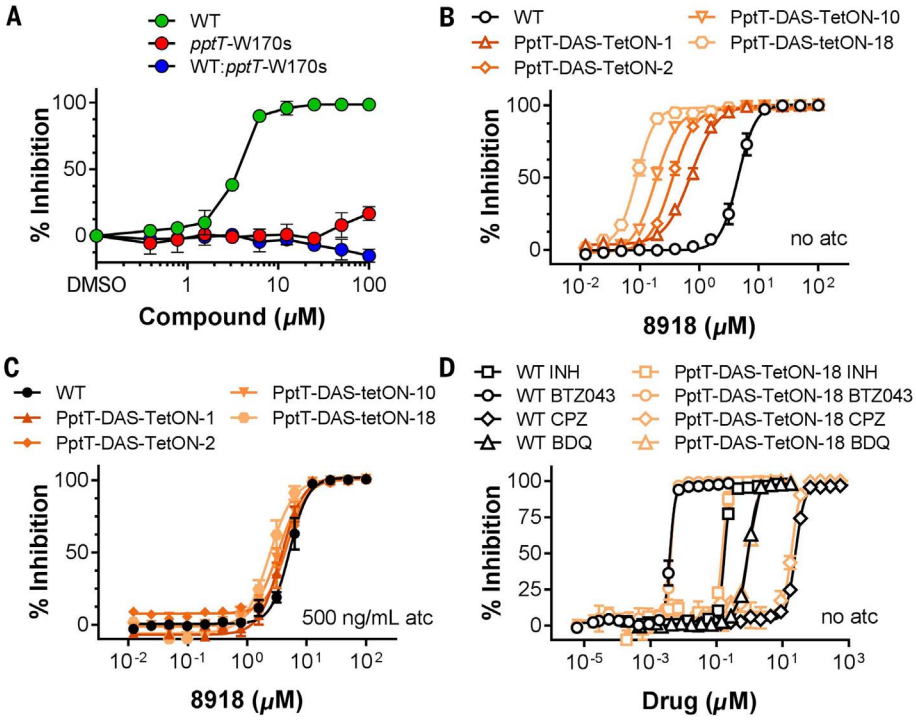

Fig. 3. Functional relevance of PptT as the target for the antimycobacterial activity of 8918. (**A**) Resistance of *pptT* mutant Mtb to 8918. Inhibition of growth of WT Mtb by 8918 but not of the *pptT* mutant W170S or WT Mtb expressing the *pptT* W170S mutant. Results are means ± SD of triplicates in one experiment representative of five. (**B**) Increased susceptibility of Mtb to growth inhibition by 8918 upon knockdown of PptT in four different strains. The degree of sensitization to 8918 correlates with the extent of the knockdown. Results are means ± SEM of at least 12 data points from four independent experiments. (**C**) Complementation with atc (anhydrotetracyline). Results are means ± SEM of at least five data points from two independent experiments. (**D**) Knockdown of PptT does not affect the potency of isoniazid (INH), BTZ043, chlorpromazine (CPZ), or bedaquiline (BDQ). Results are means ± SEM of at least five data points from two independent experiments.

which bound both 8918 and the adenosine 3′,5′-bisphosphate [phosphoadenosine phosphate (PAP)] portion of CoA (Fig. 4, C to F), which must have come from *E. coli* during preparation of recombinant PptT (*10*). Clear electron density for the inhibitor (Fig. 4C) was located in a deep hydrophobic pocket within the PptT active site (Fig. 4, D and E), where the Ppt arm of CoA resides in PptT CoA structures. The binding pocket is formed by residues Lys^{156}, Tyr^{160}, Leu^{171}, and Phe^{173} and capped by Trp^{170} (Fig. 4D), the residue whose mutation conferred high-level resistance to 8918. Trp^{170} is highly conserved among *Mycobacteria* but not in most other species (fig. S12). Glu^{157}, the catalytic base, is oriented toward the hydrophobic pocket (Fig. 4D), similar to what is observed in one of the CoA-bound structures (4QJK) (*10*). In the observed conformation for Glu^{157}, the enzyme would not be catalytically active. This contrasts with the conformation observed in 4QVH, a second PptT-CoA structure, which likely represents the physiologically active conformation of the enzyme. The carbonyl of Leu^{171} forms a H-bond with 8918. Leu^{171} forms a similar H-bond with the Ppt arm of CoA in the reported structures of CoA-bound PptT. The structure helps explain why proguanil and lidamidine are weaker inhibitors of PptT than 8918 (fig. S13). Modeling suggests that proguanil's terminal isopropyl group does not fit in the deeper portion of the hydrophobic pocket, where it would clash with Tyr^{160} (0.46 Å), Leu^{171} (0.78 Å), Gly^{172} (0.78 Å), and Phe^{173} (0.43 Å) (fig. S14A). Similarly, lidamidine's weaker action against PptT can be rationalized by its loss of van der Waals contacts with groups in the hydrophobic pocket (fig. S14B).

The presence of 8918 within the Ppt binding pocket, together with the knowledge that PptT copurifies with tightly bound CoA (*10*) and the visualization of the PAP portion of CoA, suggested that 8918 displaces the Ppt arm of CoA from the Ppt pocket. The lack of electron density for the Ppt portion of CoA is likely explained by it becoming disordered in the active site. Indeed, after incubating excess 8918 with purified PptT and denaturing the enzyme, we recovered intact CoA, not PAP (fig. S15). The same was true when we extracted PptT-8918 cocrystals (fig. S16). Moreover, 8918 does not require catalytic turnover of CoA to bind PptT, because 8918 inhibited the single turnover that the purified enzyme carried out using only the CoA with which it copurified (fig. S17). Thus, 8918 does not displace CoA from PptT but does displace the Ppt arm of CoA from its binding pocket rather than occupying a pocket that is vacant as a result of prior cleavage of Ppt from CoA to generate PAP. Displacement of CoA's Ppt arm from its ideal position by 8918 decreases but does not abolish PptT's catalytic activity. This likely explains why inhibition by 8918 is noncompetitive and incomplete.

Loss of function of Rv2795c confers resistance to 8918

Concentrations of 8918 that afforded only partial inhibition of PptT were extensively mycobactericidal. This led us to hypothesize that an endogenous inhibitor or antagonist of PptT may augment the action of 8918.

The hypothetical protein encoded by *rv2795c* is predicted to be a potential phosphohydrolase (fig. S18). It is rare for mutations in the coding sequence of an enzyme to increase its function, yet many different mutations in Rv2795c produced the same resistance phenotype. Thus, it seemed likely that resistance arose through LOF. The point mutations in *rv2795c* that conferred resistance were indeed LOF mutations because knockout of *rv2795c* produced the same phenotype: The Δ*rv2795c* strain grew normally yet was highly and selectively resistant to 8918 (Fig. 5A). Expression of WT *rv2795c* in the Δ*rv2795c* strain fully restored sensitivity to 8918, whereas complementation of the knockout with the H246N mutant did not (Fig. 5A). Finally, the H246N point mutation in *rv2795c* did not affect the level of *pptT* transcripts (fig. S19). The resistance of Mtb with a LOF of *rv2795c* was also manifest in primary mouse bone marrow–derived macrophages, where 8918 killed WT Mtb but not the *rv2795c* knockout (fig. S20). LOF of a nonessential protein can impart resistance to a bactericidal agent if the WT protein augments accumulation of the antibacterial agent in the cell or converts it from a prodrug form to its active form. However, when 8918 was tracked as an analyte in the study of its impact on Mtb's metabolome, we found that 8918 accumulated to a comparable extent and in unmodified form in WT Mtb and in an Mtb clone whose resistance to 8918 was associated with mutation in *rv2795c* (fig. S21). Thus, there must be a previously undescribed mechanism of resistance arising through LOF. We turned next to biochemical studies on recombinant Rv2795c.

Rv2795c is a Ppt hydrolase

Pathways have been discovered for the regeneration of modified forms of the coenzymes biotin, pyridoxal 5′-phosphate, and thiamine (*23*). Gammaproteobacteria such as *E. coli* encode enzymes that can act in vitro as ACP phosphohydrolases, releasing 4′-Ppt from holo-ACPs (Fig. 5B). However, that in vitro reaction has been described as physiologically implausible (*24*), and it has been unknown whether the reaction takes place in cells (*25*). Mtb's genome encodes no sequence homologs of AcpH. However, we speculated that an enzyme that removes Ppt from ACPs could sensitize Mtb to inhibition of PptT and thereby augment 8918's antimycobacterial effect. This activity could explain why LOF of Rv2795c conferred resistance.

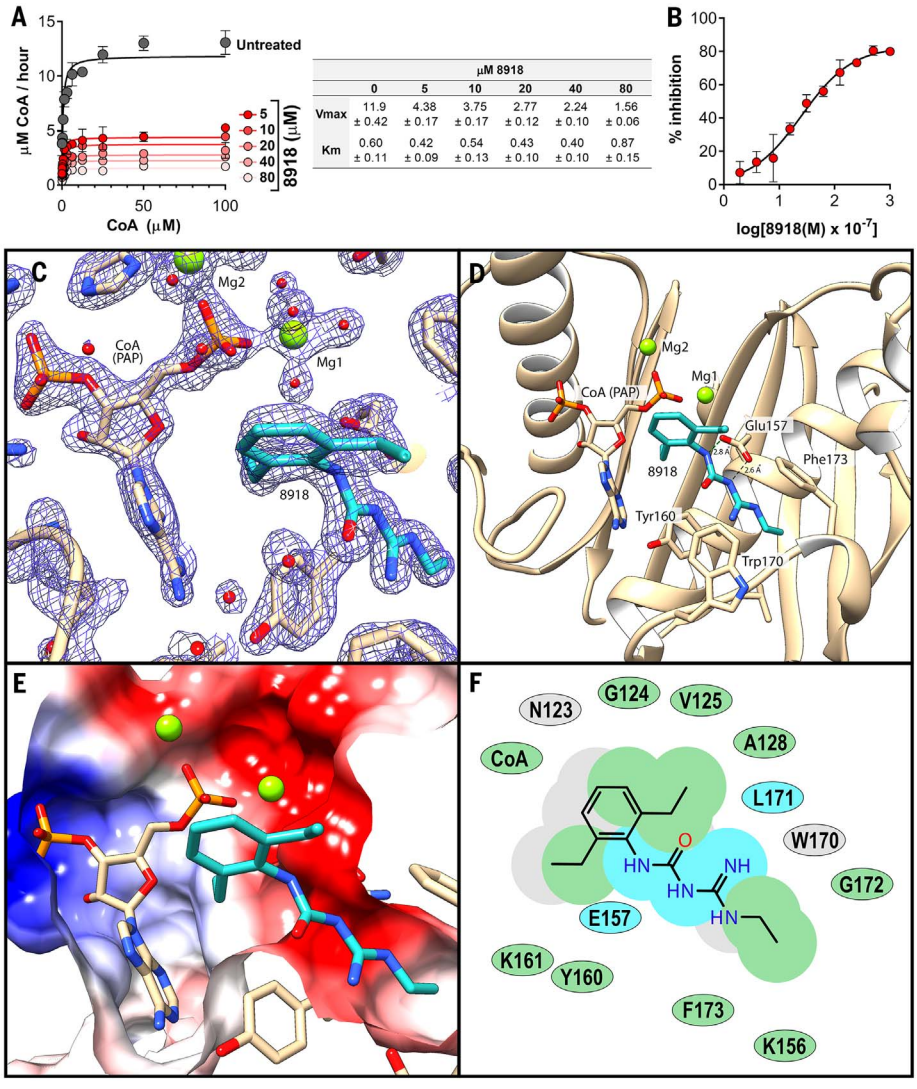

Fig. 4. Inhibition of PptT through binding of 8918 to the Ppt channel in the active site. (**A** and **B**) Impact of 8918 on activity of purified recombinant PptT. (A) V_{max} for recombinant PptT in the absence of 8918 (gray) or with 8918 at 5, 10, 20, 40, or 80 μM (shown in decreasing intensities of red). The chart displays V_{max} (in micromolar CoA per hour) and K_m (in micromolar) ± SE as a function of 8918 concentration. (B) Inhibition of PptT by 8918. IC_{50} was 2.5 μM, with maximum inhibition of 82%. Error bars indicate SD. (**C** to **F**) Structure of PptT with 8918 and adenosine 3′,5′-bisphosphate (PAP) moiety of CoA. (C) Simulated annealing composite omit electron density map (contoured at 2σ) of the PptT hydrophobic pocket showing protein residues in the active site with 8918 and PAP. (D) Active site of PptT with residues forming the Ppt binding pocket depicted with beige carbon atoms. 8918 forms van der Waals interactions with Tyr^{160}, Phe^{173}, and Trp^{170}. Glu^{157} is oriented toward the hydrophobic pocket and hydrogen bonds with 8918. Mg ions are depicted as green spheres. (E) Slice through the molecular surface of the active site of PptT colored according to the electrostatic potential (±10 kT/e). (F) two-dimensional interaction map indicating 8918's interactions with PptT. Green shading represents hydrophobic regions, blue shading represents hydrogen bond interactions, and gray shading represents accessible surface area. Single-letter abbreviations for amino acid residues: A, Ala; E, Glu; F, Phe; G, Gly; K, Lys; L, Leu; N, Asn; V, Val; W, Trp; and Y, Tyr.

To test whether Rv2795c might be a functional homolog of AcpH, we purified recombinant AcpM, an ACP that is one of PptT's native substrates in Mtb (*12*), and recombinant Rv2795c, after deleting the C-terminal 20 amino acids to improve its solubility upon overexpression in *E. coli*. Truncated recombinant Rv2795c catalyzed the conversion of holo-AcpM to apo-AcpM, as visualized by a gel shift (Fig. 5C) and confirmed by peptide mass fingerprinting of the excised bands. No conversion was detectable over the same time period in the absence of Rv2795c.

The conversion of holo- to apo-AcpM was accompanied by release of Ppt (Fig. 5D), detected by liquid chromatography–mass spectrometry (LC-MS) as an increase in an AMRT (accurate-mass, retention time) component with a m/z of 339.074 (M-H-H_2O) or 357.0891 (M-H) and an observed mass error of <5 parts per million that coeluted with a tetradeuterated standard that we synthesized and spiked into the reaction mixture (fig. S22). The standard's own identity was confirmed by proton nuclear magnetic resonance (NMR) spectroscopy (fig. S23A), MS (fig. S23B), and tandem MS (MS/MS) (fig. S23C). Free Ppt was observed with neither AcpM nor PptH alone but only with their combination. Peak amounts of Ppt were detected at the earliest time point at which the reaction could be terminated; changes occurring in free Ppt, perhaps including its cyclization or oxidation, led to time-dependent reduction in signal, precluding stoichiometric quantitation (Fig. 5D). Consistent with the hypothesis that Rv2795c is not a target of 8918, the conversion reaction catalyzed by Rv2795c was unaffected by the presence of 15 μM 8918. Accordingly, we propose that Rv2795c is a Ppt hydrolase (PptH).

Discussion

A central concept of antibiotic research is that small chemical compounds can have specific biological targets and can serve as tools to identify those targets' functions. In the present study, an inhibitor of one enzyme, PptT, led to discovery of another enzyme, PptH, that is not the inhibitor's target. Studies throughout the antibiotic era have compiled a list of seven mechanisms of antimicrobial resistance (*2*): mutation or posttranslational modification of the target that reduces binding of the drug but preserves function of the target, increased expression of the target, modification or increased catabolism of the drug, decreased activation of the prodrug, decreased drug uptake or increased drug export, or expression of a compensatory pathway. The present work adds an eighth mechanism: LOF in an enzyme that undoes the action targeted by the inhibitor.

Our findings demonstrate that PptT, a long-sought target for antimycobacterial drug discovery, can be selectively inhibited by a druglike compound. Moreover, the action of PptH makes Mtb vulnerable even to partial inhibition of PptT, such that 90% of an Mtb population could be killed by 8918 at concentrations that inhibited recombinant PptT by 37%. Resistance due to coding region mutations in PptT or PptH arose infrequently (3×10^{-7}). It is unlikely that resistance to a PptT inhibitor would arise by up-regulation of expression of the operon encoding PptT, as this would up-regulate PptH as well, further enhancing the action of the inhibitor. Judging from the impact on Mtb's synthesis of trehalose mycolates and PDIMs and consistent with the literature (*13*), inhibition of PptT appears to result in failure to activate other enzymes whose products are critical for Mtb's cell wall, virulence, and survival.

A 24-hour exposure of Mtb to 8918 also led to accumulation of a substrate of CoaBC and depletion of products of CoaBC. Those observations are consistent with inhibition of CoaBC, an essential

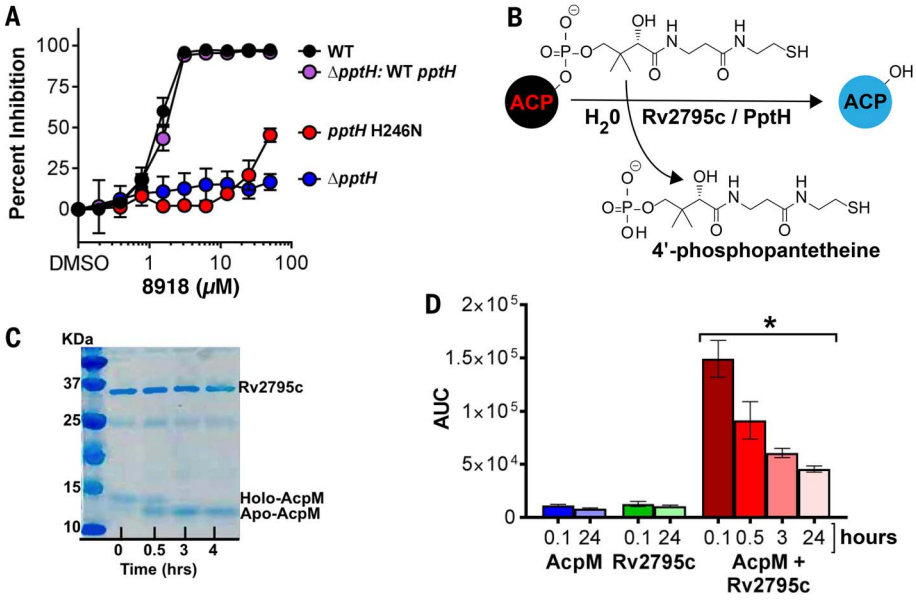

Fig. 5. Resistance to 8918 from LOF mutations in Rv2795c and identification of Rv2795c as a PptH. (**A**) Resistance to 8918 in the *rv2795c* mutant H246N and *rv2795c* knockout and restoration of sensitivity with complementation of the knockout with the WT allele to a level matching that of WT Mtb. Results are means ± SD of triplicates in one experiment representative of three. (**B**) Schematic of the reaction carried out in vitro by AcpHs. (**C** and **D**) Reaction detection with Rv2795c (PptH), which is not homologous to AcpH. (C) Conversion of holo-AcpM to apo-AcpM on incubation with C-terminally truncated Rv2795c for up to 4 hours. The results shown are representative of five experiments. (D) Detection of Ppt during incubation of AcpM alone, Rv2795c alone, or the combination over the number of hours indicated. The results shown are representative of three experiments. The asterisk indicates statistically significant differences at all time points from each of the controls ($P < 0.002$ for the 0.1-hour time point; unpaired Student's *t* test). Decreasing recovery of Ppt with time reflects instability of the compound. AUC, area under the curve (ion counts).

enzyme (*4*) that catalyzes the conjugation of cysteine to 4′-phosphopantothenate and decarboxylates the resulting 4-phosphopantothenoylcysteine to form 4'-phosphopantetheine. Further study is needed to determine whether CoaD, CoaE, and/or CoaBC are inhibited after exposure of Mtb to 8918, and if so, the mechanism(s) through which inhibition is mediated (*26*). However, the primacy of PptT as the functionally critical target of 8918 was evident from the occurrence of preservation-of-function mutations in *pptT* or LOF mutations *pptH* in all 12 8918-resistant clones of Mtb and all 12 8918-resistant clones of *M. smegmatis* that we isolated, the conferral of resistance as a dominant phenotype upon expression of the mutant *pptT* allele, and the marked increase in sensitivity to 8918 upon knockdown of PptT.

The cocrystal structure of the PptT-8918-CoA complex helps explain both the noncompetitive mode of inhibition by 8918 and the incompleteness of inhibition. The inhibitor's amidino-urea moiety occupies the hydrophobic binding pocket that normally accommodates the Ppt arm of CoA, displacing the Ppt from its ideal position for catalysis without displacing CoA.

The amidino-urea compound we identified was active against Mtb in vitro and in Mtb-infected mice while sparing other microorganisms and mammalian cells. A narrow-spectrum agent is highly desirable for treatment of TB, both to avoid dysbiosis with prolonged treatment and to discourage use as monotherapy for other infections, which could hasten the emergence of drug resistance in people with undiagnosed TB.

In 1967, Vagelos and Larrabee partially purified an enzyme from *E. coli* that cleaved Ppt from an ACP in vitro and called it AcpH (*27*). In 2005, Thomas and Cronan identified the gene encoding AcpH, as confirmed by the activity of the recombinant protein (*24*). They speculated that AcpH must not have such an action in vivo, because "the cellular content of AcpH activity is sufficient to hydrolyze all of the cellular ACP in <1 min…the physiologic role of AcpH remains enigmatic" (*24*). Indeed, the AcpH reaction has not been demonstrated to take place in a cell. Investigation of the basis of resistance to the PptT inhibitor provides evidence that an enzyme functions in an intact cell to remove Ppt from holo-ACPs. Mtb's Rv2795c bears no homology to bacterial AcpHs (*28*, *29*); hence, a different name seems warranted—PptH. PptH is conserved among mycobacteria, including *Mycobacterium leprae*, despite severe genomic reduction in *M. leprae*, suggesting a crucial function in this genus. The discovery of PptH as an enzyme that functions within Mtb to undo the PptT reaction elevates the enigma from a hypothetical to an imperative for investigating a seemingly self-destructive reaction in CoA metabolism that presumably serves a physiologic role.

Materials and methods summary

Full details are provided in the supplementary materials.

High-throughput screen and antimycobacterial assays

The initial screen was conducted against the auxotrophic Mtb strain mc^{2}6220 (Δ*panCD*Δ*lysA*) from W. R. Jacobs Jr., Albert Einstein College of Medicine. All experiments whose results are presented in the figures were performed with Mtb H37Rv.

Antimicrobial spectrum and cytotoxicity assays

E. coli, *P. aeruginosa*, *S. aureus*, and *C. albicans* were clinical isolates from NewYork-Presbyterian Hospital. The *Streptomyces* species *S. coelicolor*, *S. roseosporus*, *S. antibioticus*, and *S. albidoflavus* were gifts from Sean Brady, Rockefeller University. Mammalian cell cytotoxicity was evaluated by measuring ATP content with the CellTiterGlo luminescence assay (Promega) in HepG2 human hepatocarcinoma cells after 40 hours of incubation with a test agent.

Treatment of Mtb-infected mice

Mouse treatment procedures were approved by the Animal Care and Use Committee of Sanofi. Female BALB/c mice aged 5 to 7 weeks were rested 1 week before infection, inoculated intranasally with 10^6 H37Rv Mtb, treated by gavage beginning 1 day later for 4 days per week, and euthanized 1 day after receiving the eighth dose. Lung homogenates were plated for CFU.

Mutant selection of 8918-resistant Mtb and Mycobacterium smegmatis

Bacteria (10^8 and 10^7 cells) were plated on 7H11 agar at 4× and 8× the MIC. Surviving colonies were restreaked on 7H11 plates containing 0.2% glycerol, 10% OADC, and 12.5 μM 8918 to confirm resistance.

Metabolomics

Mtb was grown to OD_{580} = 1 in 7H9. One ml was added to each nylon Durapore 0.22-μm membrane filter. Filters were placed on Middlebrook 7H11 agar supplemented with 0.2% glycerol and 10% OADC, incubated at 37°C for 1 week to expand the biomass, and transferred to lay atop a reservoir containing 7H9 medium with 0.2% glycerol (no tyloxapol) and varied concentrations of test agent. After 24 or 48 hours at 37°C, filters were extracted with 40:40:20 methanol:acetonitrile:water in a bead beater. Lysates were mixed with equal volumes of 50% acetonitrile and 0.2% formic acid for MS in positive- and negative-ion mode (*16*).

Thin-layer chromatography

Cultures of *Mycobacterium bovis* var. Bacille Calmette-Guérin (BCG) were incubated with

8918, proguanil, or isoniazid for 12 hours and then exposed to ^{14}C acetate or ^{14}C propionate for 24 hours. Lipids were extracted with methanol and chloroform, dried, and subjected to chromatography on silica gels as described (*30*).

Lipidomics

Cell mats prepared as for metabolomics were placed on reservoirs with test agents for 24 hours, then sequentially extracted with mixtures of chloroform:methanol, evaporated, and resuspended in 70:30 [v/v] hexane:isopropanol, 0.02% formic acid [m/v], and ammonium hydroxide 0.01% [m/v] for MS (*31*).

Protein purification

His-tagged PptT, apo-BpsA (*Streptomyces lavendulae* blue pigment synthetase A), AcpM, and Rv2795c (lacking the 20 amino acids after residue 304) were expressed in *E. coli* BL21 cells (Invitrogen) and purified on a Ni-NTA resin for enzyme assays. For crystallization, PptT was further purified by size exclusion chromatography.

Enzyme assays

PptT's ability to phosphopantetheinylate apo-BpsA was measured by the ability of the resulting holo-BpsA to convert two molecules of L-glutamine into one molecule of indigoidine, which absorbs light at 590 nm (*21*, *22*). Rv2795c (5 μM) and AcpM (10 μM) were combined along with a synthetic tetradeuterated PptT standard for the indicated times, the mixture centrifuged through a 10,000 molecular weight cut-off filter, and the filtrate analyzed by LC-MS. Alternatively, the reaction mixture was boiled in SDS–polyacrylamide gel electrophoresis (PAGE) loading dye and subjected to SDS-PAGE.

Crystallization of PptT

PptT was incubated with excess 8918 and screened against Hampton research crystallization conditions (*32*). The most promising condition was optimized by varying the pH and precipitant concentration using vapor diffusion (*33*). X-ray diffraction data were collected at APS Argonne National Labs. The structure was solved with molecular replacement (*34*) using reported PptT structures 4QJK (*10*) and 4QVH (*9*) as search models.

Construction of PptT knockdown strains

SspB-controlled proteolysis was used to conditionally deplete PptT (*18*–*20*). First, *pptT* was first tagged in situ with a DAS-tag (*18*–*20*). The resulting *Mtb* strain was transformed with four plasmids (TetON-1, TetON-2, TetON-10, TetON-18), which, upon removal of anhydrotetracyline (atc), produce different levels (TetON-18 > TetON-10 > TetON-2 > TetON-1) of the DAS-recognition protein SspB and thus mediate graded depletion of PptT-DAS.

Chemistry

N-[(2,6-Diethylphenyl)carbamoyl]acetamide (compound 8918) was synthesized from 1-ethylguanidine and 2,6-diethylphenyl isocyanate using modifications of published protocols (*35*, *36*). Tetradeuterated Ppt standard (Ppt-d4) was synthesized by condensation of pantothenic acid with tetradeuterated, protected 2-mercaptoethylamine, followed by phosphorylation of the primary alcohol, removal of protecting groups, and high-performance liquid chromatography purification to >98%, as demonstrated by evaporative light scattering, ultraviolet detection, and MS. Proton NMR analysis in argon-degassed D_2O was consistent with deuteration above 98%, and ^{31}P NMR revealed a single phosphorus peak.

Statistical analysis

Groups were compared by analysis of variance (ANOVA) or Student's unpaired *t* test as described in the legends.

REFERENCES AND NOTES

1. C. Walsh, Molecular mechanisms that confer antibacterial drug resistance. *Nature* **406**, 775–781 (2000). doi: 10.1038/35021219; pmid: 10963607
2. C. Nathan, Kunkel Lecture: Fundamental immunodeficiency and its correction. *J. Exp. Med.* **214**, 2175–2191 (2017). doi: 10.1084/jem.20170637; pmid: 28701368
3. P. Sukheja *et al*., A novel small-molecule inhibitor of the *Mycobacterium tuberculosis* demethylmenaquinone methyltransferase MenG is bactericidal to both growing and nutritionally deprived persister cells. *mBio* **8**, e02022-16 (2017). doi: 10.1128/mBio.02022-16; pmid: 28196957
4. J. C. Evans *et al*., Validation of CoaBC as a bactericidal target in the coenzyme A pathway of *Mycobacterium tuberculosis*. *ACS Infect. Dis.* **2**, 958–968 (2016). doi: 10.1021/acsinfecdis.6b00150; pmid: 27676316
5. W. J. Moolman, M. de Villiers, E. Strauss, Recent advances in targeting coenzyme A biosynthesis and utilization for antimicrobial drug development. *Biochem. Soc. Trans.* **42**, 1080–1086 (2014). doi: 10.1042/BST20140131; pmid: 25110006
6. K. J. Saliba, C. Spry, Exploiting the coenzyme A biosynthesis pathway for the identification of new antimalarial agents: The case for pantothenamides. *Biochem. Soc. Trans.* **42**, 1087–1093 (2014). doi: 10.1042/BST20140158; pmid: 25110007
7. C. Spry, K. Kirk, K. J. Saliba, Coenzyme A biosynthesis: An antimicrobial drug target. *FEMS Microbiol. Rev.* **32**, 56–106 (2008). doi: 10.1111/j.1574-6976.2007.00093.x; pmid: 18173393
8. K. Gokulan, A. Aggarwal, L. Shipman, G. S. Besra, J. C. Sacchettini, *Mycobacterium tuberculosis* acyl carrier protein synthase adopts two different pH-dependent structural conformations. *Acta Crystallogr. D* **67**, 657–669 (2011). doi: 10.1107/S0907444911020221; pmid: 21697604
9. J. Jung *et al*., Crystal structure of the essential *Mycobacterium tuberculosis* phosphopantetheinyl transferase PptT, solved as a fusion protein with maltose binding protein. *J. Struct. Biol.* **188**, 274–278 (2014). doi: 10.1016/j.jsb.2014.10.004; pmid: 25450595
10. C. R. Vickery *et al*., Structure, biochemistry, and inhibition of essential 4′-phosphopantetheinyl transferases from two species of Mycobacteria. *ACS Chem. Biol.* **9**, 1939–1944 (2014). doi: 10.1021/cb500263p; pmid: 24963544
11. P. J. Brennan, Structure, function, and biogenesis of the cell wall of *Mycobacterium tuberculosis*. *Tuberculosis* **83**, 91–97 (2003). doi: 10.1016/S1472-9792(02)00089-6; pmid: 12758196
12. O. Zimhony *et al*., AcpM, the meromycolate extension acyl carrier protein of *Mycobacterium tuberculosis*, is activated by the 4′-phosphopantetheinyl transferase PptT, a potential target of the multistep mycolic acid biosynthesis. *Biochemistry* **54**, 2360–2371 (2015). doi: 10.1021/bi501444e; pmid: 25785780
13. C. Leblanc *et al*., 4′-Phosphopantetheinyl transferase PptT, a new drug target required for *Mycobacterium tuberculosis* growth and persistence in vivo. *PLOS Pathog.* **8**, e1003097 (2012). doi: 10.1371/journal.ppat.1003097; pmid: 23308068
14. G. L. Abrahams *et al*., Pathway-selective sensitization of *Mycobacterium tuberculosis* for target-based whole-cell screening. *Chem. Biol.* **19**, 844–854 (2012). doi: 10.1016/j.chembiol.2012.05.020; pmid: 22840772
15. Z. Xu *et al*., Reaction intermediate analogues as bisubstrate inhibitors of pantothenate synthetase. *Bioorg. Med. Chem.* **22**, 1726–1735 (2014). doi: 10.1016/j.bmc.2014.01.017; pmid: 24507827
16. M. Nandakumar, G. A. Prosser, L. P. de Carvalho, K. Rhee, Metabolomics of *Mycobacterium tuberculosis*. *Methods Mol. Biol.* **1285**, 105–115 (2015). doi: 10.1007/978-1-4939-2450-9_6; pmid: 25779312
17. M. A. DeJesus *et al*., Comprehensive essentiality analysis of the *Mycobacterium tuberculosis* genome via saturating transposon mutagenesis. *mBio* **8**, e02133-16 (2017). doi: 10.1128/mBio.02133-16; pmid: 28096490
18. J. H. Kim *et al*., A genetic strategy to identify targets for the development of drugs that prevent bacterial persistence. *Proc. Natl. Acad. Sci. U.S.A.* **110**, 19095–19100 (2013). doi: 10.1073/pnas.1315860110; pmid: 24191058
19. J. H. Kim *et al*., Protein inactivation in mycobacteria by controlled proteolysis and its application to deplete the beta subunit of RNA polymerase. *Nucleic Acids Res.* **39**, 2210–2220 (2011). doi: 10.1093/nar/gkq1149; pmid: 21075796
20. D. Schnappinger, K. M. O'Brien, S. Ehrt, Construction of conditional knockdown mutants in mycobacteria. *Methods Mol. Biol.* **1285**, 151–175 (2015). doi: 10.1007/978-1-4939-2450-9_9; pmid: 25779315
21. A. S. Brown, K. J. Robins, D. F. Ackerley, A sensitive single-enzyme assay system using the non-ribosomal peptide synthetase BpsA for measurement of L-glutamine in biological samples. *Sci. Rep.* **7**, 41745 (2017). doi: 10.1038/srep41745; pmid: 28139746
22. J. G. Owen, J. N. Copp, D. F. Ackerley, Rapid and flexible biochemical assays for evaluating 4′-phosphopantetheinyl transferase activity. *Biochem. J.* **436**, 709–717 (2011). doi: 10.1042/BJ20110321; pmid: 21466506
23. C. L. Linster, E. Van Schaftingen, A. D. Hanson, Metabolite damage and its repair or pre-emption. *Nat. Chem. Biol.* **9**, 72–80 (2013). doi: 10.1038/nchembio.1141; pmid: 23334546
24. J. Thomas, J. E. Cronan, The enigmatic acyl carrier protein phosphodiesterase of *Escherichia coli*: Genetic and enzymological characterization. *J. Biol. Chem.* **280**, 34675–34683 (2005). doi: 10.1074/jbc.M505736200; pmid: 16107329
25. J. Thomas, D. J. Rigden, J. E. Cronan, Acyl carrier protein phosphodiesterase (AcpH) of *Escherichia coli* is a non-canonical member of the HD phosphatase/phosphodiesterase family. *Biochemistry* **46**, 129–136 (2007). doi: 10.1021/bi061789e; pmid: 17198382
26. Y. Abiko, Investigations on pantothenic acid and its related compounds. X. Biochemical studies. 5. Purification and substrate specificity of phosphopantothenoylcysteine decarboxylase from rat liver. *J. Biochem.* **61**, 300–308 (1967). doi: 10.1093/oxfordjournals.jbchem.a128548; pmid: 6061681
27. P. R. Vagelos, A. R. Larrabee, Acyl carrier protein. IX. Acyl carrier protein hydrolase. *J. Biol. Chem.* **242**, 1776–1781 (1967). pmid: 4290442
28. N. M. Kosa, K. M. Pham, M. D. Burkart, Chemoenzymatic exchange of phosphopantetheine on protein and peptide. *Chem. Sci.* **5**, 1179–1186 (2014). doi: 10.1039/C3SC53154F; pmid: 26998215
29. E. Murugan, R. Kong, H. Sun, F. Rao, Z. X. Liang, Expression, purification and characterization of the acyl carrier protein phosphodiesterase from *Pseudomonas Aeruginosa*. *Protein Expr. Purif.* **71**, 132–138 (2010). doi: 10.1016/j.pep.2010.01.007; pmid: 20064615
30. W. Li *et al*., Novel insights into the mechanism of inhibition of MmpL3, a target of multiple pharmacophores in *Mycobacterium tuberculosis*. *Antimicrob. Agents Chemother.* **58**, 6413–6423 (2014). doi: 10.1128/AAC.03229-14; pmid: 25136022
31. E. Layre *et al*., A comparative lipidomics platform for chemotaxonomic analysis of *Mycobacterium tuberculosis*. *Chem. Biol.* **18**, 1537–1549 (2011). doi: 10.1016/j.chembiol.2011.10.013; pmid: 22195556
32. J. Jancarik, S.-H. Kim, Sparse matrix sampling: A screening method for crystallization of proteins. *J. Appl. Cryst.* **24**, 409–411 (1991). doi: 10.1107/S0021889891004430
33. B. Zheng, J. D. Tice, L. S. Roach, R. F. Ismagilov, A droplet-based, composite PDMS/glass capillary microfluidic system for evaluating protein crystallization conditions by microbatch and vapor-diffusion methods with on-chip X-ray diffraction. *Angew. Chem. Int. Ed.* **43**, 2508–2511 (2004). doi: 10.1002/anie.200453974; pmid: 15127437
34. G. Bunkóczi *et al*., Phaser.MRage: Automated molecular replacement. *Acta Crystallogr. D* **69**, 2276–2286 (2013). doi: 10.1107/S0907444913022750; pmid: 24189240

35. S. Muzi, S. Abdul-Rahman, "Novel compounds, specifically aromatic and heteroaromatic ureas and thioureas, useful against parasites and especially against coccidiosis." Patent WO 2001030749 A1 (2001).
36. Q. Zhang *et al*., Unambiguous synthesis and prophylactic antimalarial activities of imidazolidinedione derivatives. *J. Med. Chem.* **48**, 6472–6481 (2005). doi: 10.1021/jm0504252; pmid: 16190773
37. E. Ballinger *et al*., PDB ID 6CT5, Protein Data Bank (2019); http://dx.doi.org/10.2210/pdb6CT5/pdb.

ACKNOWLEDGMENTS

We thank M. Nandakumar, T. Lupoli, T. Warrier, D. Zhang, D. Little, J. Roberts, Y. Ling, M. Wood, L. Lopez-Quezada, X. Jiang, and O. Ocheretina (Weill Cornell Medicine); M. Blaise (Aarhus University); L. Kremer (Université de Montpellier II); J. Bean (Sloan Kettering Institute); B. Neuenswander (University of Kansas); S. Brady (Rockefeller University); V. Dartois and members of her laboratory (Rutgers University); H. Boshoff and C. E. Barry III (NIAID); B. Wan and S. Franzblau (University of Illinois); and M. Glickman (Sloan Kettering Institute) for contributing advice, reagents, or assistance with experiments. We thank M. B. Barrio (Sanofi) for collaboration at the outset of screening, E. Leberer (Sanofi) for alliance management, and the Midwest Center for Structural Genomics for contributing LIC vectors. Results described in this report are derived from work performed at Argonne National Laboratory, Structural Biology Center (SBC), at the Advanced Photon Source. SBC-CAT is operated by UChicago Argonne, LLC, for the U.S. Department of Energy, Office of Biological and Environmental Research, under contract DE-AC02-06CH1135. We thank the staff at beamline 19-ID and 23-ID of the APS at Argonne National Labs and the Laboratory of Biological Mass Spectrometry, Texas A&M University (D. Kim), for assisting with the LC-MS/MS analysis of CoA bound to PptT; the Integrated Metabolomics Analysis Core (IMAC), Texas A&M University (C. Klemashevich), for assisting with the LC-MS/MS analysis of the dissolved PptT 8918 cocrystals; and A. Silva (Texas A&M) for assistance with equilibrium dialysis studies. **Funding:** This work was funded by the Tri-Institutional TB Research Unit grant U19AI-111143 from the National Institute of Allergy and Infectious Diseases (NIAID) (C.N.), the Abby and Howard P. Milstein Program in Chemical Biology and Translational Medicine (C.N.), grant A-0015 from the Welch Foundation (J.S.), TB Structural Genomics grant P01AI095208 from NIAID (J.S.), and a grant from the Bill and Melinda Gates Foundation (D.S.). The Organic Synthesis Core is partially supported by NCI Core Grant P30 CA008748. The Weill Cornell Department of Microbiology and Immunology is supported by the William Randolph Hearst Foundation. **Author contributions:** E. Bal., J.M., T.H., R.M., I.B., K.M., K.B.-H., J.V., A.F., C.A.E., and J.A.M. performed experiments. S.M.S. and G.Y. synthesized compounds. T.R.I. sequenced resistant mutants. C.R., L.G., S.S., C.C., S.L., E. Bac., and L.F. provided the screening deck and helped oversee the project. K.B.-H., B.G., D.S., and K.R. provided critical advice. J.S. supervised the enzymology, crystallography, and sequencing. J.A. and O.O. supervised the chemistry. K.R. supervised the metabolomics and lipidomics. D.S. supervised the genetics. C.N. organized the project and supervised the microbiology. E.B., J.M., J.S., and C.N. wrote the paper, with contributions to the materials and methods section by I.B., S.M.S., J.A., D.S., O.O., B.G., K.B.-H., and J.V. **Competing interests:** L.G., I.B., S.L., L.F., C.C., E.Bac, and C.R. were employees of Sanofi, Inc. The authors declare no other competing interests. No patent on 8918 has been filed. C.N. declares noncompeting service on the scientific advisory boards of the Global Alliance for TB Drug Development, the Board of Governors of the Tres Cantos Open Lab Foundation, the Pfizer Centers for Therapeutic Innovation National Therapeutic Area Panel, and Leap Therapeutics. **Data and materials availability:** All data to support the conclusions of this manuscript are included in the main text, supplementary materials, and the Protein Data Bank (PDB 6CT5) (*37*). All materials are available on request, including chemical compounds as supplies permit, subject to a standard material transfer agreement.

SUPPLEMENTARY MATERIALS

1 August 2018; accepted 21 December 2018
10.1126/science.aau8959